CERN-INTC-2017-040 / INTC-P-511
31/05/2017

EUROPEAN ORGANIZATION FOR NUCLEAR RESEARCH

Proposal to the ISOLDE and Neutron Time-of-Flight Committee

The structure of the low-lying excited states in ^{182,184,186}Hg studied through β^+/EC decay of ^{182,184,186}Tl at IDS

May 31, 2017

K. Rezynkina[1], A. Algora[2], B. Andel[3], A.N. Andreyev[4], S. Antalic[3], A. Barzakh[5], T. Berry[6], H. De Witte[1], A. Esmayaldezeh[7], V.N. Fedosseyev[8], L. Gaffney[8], L. Harkness-Brennan[9], M. Huyse[1], A. Illana[1], J. Jolie[7], D. Joss[9], D. Judson[9], J. Litzinger[7], B.A. Marsh[8], L. Morrison[6], E. Nacher[10] J. Pakarinen[11,12], Z. Podolyak[6], E. Rapisarda[13], J.-M. Regis[7], M. Stryjczyk[1], Y. Tsunoda[14], O. Tengblad[10], J. Ojala [11,12], T. Otsuka[15,1], P. Van Duppen[1], N. Warr[7], K. Wrzosek-Lipska[16] and IDS collaboration

[1] *KU Leuven, Instituut voor Kern- en Stralingfysica, 3001, Leuven, Belgium*
[2] *Instituto de Fisica Corpuscular, CSIC - Universidad de Valencia, E-46071 Valencia, Spain*
[3] *Department of Nuclear Physics and Biophysics, Comenius University, 84248, Slovakia*
[4] *Department of Physics, University of York, Heslington, York, YO10 5DD, United Kingdom*
[5] *Petersburg Nuclear Physics Institute, NRC Kurchatov Institute, 188350, Gatchina, Russia*
[6] *University of Surrey, Guildford, United Kingdom*
[7] *Institut fur Kernphysik, Universitat zu Koln, D-50937 Koln, Germany*
[8] *EN Department, CERN, CH-1211 Geneve 23, Switzerland*
[9] *University of Liverpool, United Kingdom*
[10] *Instituto de Estructura de la Materia, CSIC, E-28006 Madrid, Spain*
[11] *University of Jyvaskyla, Finland*
[12] *Helsinki Institute of Physics, Finland*
[13] *Paul Scherrer Institut, Villigen, Switzerland*
[14] *Center for Nuclear Study, University of Tokyo, Hongo, Bunkyo-ku, Tokyo 113-0033, Japan*
[15] *RIKEN Nishina Center, 2-1 Hirosawa, Wako, Saitama 351-0198, Japan*
[16] *Heavy Ion Laboratory, University of Warsaw, Poland*

Spokesperson: Kseniia Rezynkina, kseniia.rezynkina@kuleuven.be
Contact person: Liam Gaffney, liam.gaffney@cern.ch

Abstract: We propose to probe the low-lying nuclear structure of ^{182,184,186}Hg populated in β^+/EC decay of ^{182,184,186}Tl by means of the combined γ-ray and internal conversion electron spectroscopy. This proposal has a four-fold aim: firstly, to determine the precise relative γ-ray branching ratios of the decays of the low-lying (yrast and non-yrast) states and the internal conversion coefficients of the ΔI=0, $I \neq$0 transitions in the ^{182,184,186}Hg. These data are an essential input for the analysis of the Coulomb excitation experiment planned with the HIE-ISOLDE. Secondly, by precisely measuring the ICC of the $2_2^+ \rightarrow 2_1^+$ transition the difference in deformation of the two states and their degree of mixing can be deduced. Thirdly, by measuring the de-excitation pattern of the 2_3^+, the hypothesis of a γ-vibrational band can be verified. Fourthly, we aim to determine the monopole strengths of the $0^+ \rightarrow 0^+$ transitions by combining the data from the decay and coulex spectroscopy.

Requested shifts: 5 shifts, (a single run)

1 Introduction

Shape coexistence is a phenomenon which occurs when states in the same nucleus at similar excitation energies display different intrinsic deformations. For the past 45 years it was found to occur in many regions across the nuclear chart: from the light $N \approx 20$ neutron-rich nuclei [1] across the region of Ni and Cu near $N = 40$ and up to the heavy nuclei near $Z = 50$ and $Z = 82$ shell closures [2].

Shape coexistence generally occurs when intruder states come down in excitation energy to the vicinity of the spherical states, yielding the low-lying non-yrast energy levels (see e.g. fig.1). The mixing between the states with the same I of the coexisting configurations gives rise to transitions with a strong electric monopole component ($\rho^2(E0) \geq 0.02$), often referred to as strong fingerprints of shape coexistence [3]. Such transitions are either highly (in case of mixed E0/M1/E2 multipolarities) or fully (for the $0^+ \rightarrow 0^+$ transitions) converted. Thus, the internal conversion electron (ICE) spectroscopy is an invaluable tool for the study of the decay properties of the shape-coexisting nuclei.

The neutron-deficient mercury isotopes ($Z = 80$) are a good example of shape coexis-

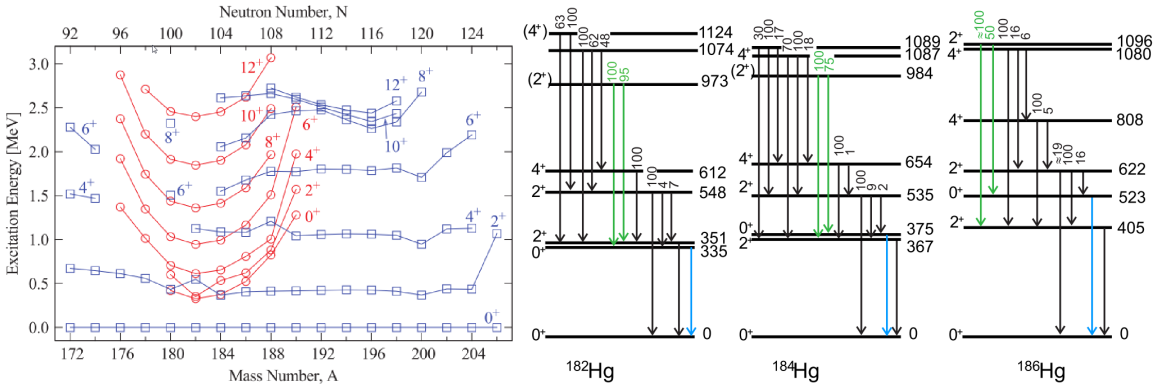

Figure 1: (Left) Level energy systematics of even-mass mercury isotopes. Red circles indicate the intruder prolate states, blue squares indicate the oblate states [4]; (Right) The simplified level schemes of ^{182,184,186}Hg with the relative γ-ray intensities of the decay of each state; the excitation energies are given in keV [5].

tence. The first evidence of the shape coexistence phenomenon in the lead region was observed through the isotope shift measurements for mercury, when ^{183}Hg and ^{185}Hg displayed a dramatic change in the ground state mean-squared charge radius $<r^2>$ compared to heavier-mass mercury isotopes [6]. The difference of the ground state charge radii between the even and odd mercury isotopes is a bright manifestation of the shape coexistence. The even-even isotopes ^{182,184,186}Hg have weekly deformed oblate ground state shapes. In contrast, the odd-even nuclei demonstrate increased charge-radii corresponding to a prolate deformation with a deformation parameter $<\beta_2^2> \sim 0.09$. It has been recently demonstrated by means of laser spectroscopy [7] that this effect, referred to as 'shape-staggering', is very local, with the increased charge-radii only found in ^{181,183,185}Hg isotopes.

Due to the proximity of $Z = 82$ shell closure, the structure of the neutron-deficient mercury isotopes is highly sensitive to the interplay between the microscopic properties of the

nucleus and the collective (macroscopic) effects. The study of these nuclei is thus a major challenge for the theorists, and the experimental knowledge of their properties is invaluable to test the predictions of various theoretical models, such as the beyond mean-field model (BMF) [8], the quadrupole collective model based on the General Bohr Hamiltonian (GBH) [9], the interacting boson based model with configuration mixing (IBM) [10]. The results of this experiment will be compared to the BMF and GBH calculations as well as to the first Monte-Carlo Shell model calculations for this region which are currently being carried out by the group of T. Otsuka.

The energy of the first excited 2^+ states and the B(E2) strength of the $2_1^+ \rightarrow 0_1^+$ transition are often used to trace the evolution of the nuclear structure. However, in $^{180-186}$Hg the energy of the yrast 2^+ level (see fig.1) as well as the B(E2) remains practically constant along the isotopic chain. Though the excitation energy remains unchanged, the mixing of the ground state band to the intruder prolate states may vary drastically between ^{182}Hg and ^{184}Hg [4]. It is thus very important to determine this mixing in order to correctly interpret the experimental data.

Coulomb excitation (coulex) experiments allow to determine transitional matrix elements, together with their relative signs, between all nuclear states populated in the experiment. Moreover, spectroscopic quadrupole moments (both magnitudes and signs) can also be obtained for various states. All these unique experimental results provide a direct probe of nuclear deformation in a given state, including information on asymmetry. Recent coulex experiment with 2.85 MeV/u beams from REX-ISOLDE (IS452) allowed to extract the electric quadrupole properties of some of the low-lying yrast and non-yrast states in the even-even $^{182-188}$Hg isotopes [11, 12]. The future experiment (IS563) using the higher energy beams of HIE-ISOLDE will give access to the higher excitations (up to 10^+ states) of ^{182,184}Hg. A set of reduced matrix elements that couple several excited states, including the not well known non-yrast states, will be extracted. However, the determination of the $< f||M(E2)||i >$ and $< f||M(M1)||i >$ matrix elements crucially requires complementary data to provide important constraints for a large set of strongly correlated matrix elements used in the coulex analysis. For instance, by decreasing the uncertainty on the branching ratios and ICC of the decay of the 2_2^+ state in ^{182}Hg from $\sim$30% to $\sim$3%, a factor of 1.5 in precision can be gained for the quadrupole moment of the 2_1^+ state.

β^+/EC decay of thallium to mercury has been previously investigated at ISOLDE (IS466 for ^{182}Tl and IS511 for ^{184}Tl) as a 'parasitic' part of a systematic β-delayed fission and laser spectroscopy study of neutron-deficient thallium isotopes [13, 14]. An identical setup was used for both experiments (see [15] for a detailed description). As this setup was optimised for the needs of laser- and β-delayed spectroscopy, the conditions for the studies of the excited states in ^{182,184}Hg were not ideal. The Si detector used for the ICE detection was operated with a threshold at $\sim$200 keV; the energy resolution was $\sim$24 keV at 300 keV; moreover, due to the limited thickness of the detector, the punch-through β electrons constituted an essential background for the ICE lines of interest. Additionally, since the Ge-detector configurations were compact, the γ-ray efficiency of the setup was affected by summing problems. Nonetheless, some spectroscopic data, such as the branching ratios and the values of the ICC for the $2_2^+ \rightarrow 2_1^+$ transitions were extracted [5]. However, for the reasons described above, the uncertainties on many of these values are rather high, which is an obstacle for the precise interpretation of the coulex data.

We thus put forward a proposal to study the ^{182,184,186}Hg isotopes populated in the β^+/EC decay of ^{182,184,186}Tl respectively by means of the combined γ & ICE spectroscopy with an optimized dedicated detector setup based on IDS. Such studies will allow us to determine the branching ratios of the transitions between the states with same I belonging to coexisting bands more accurately, as well as to extract several conversion coefficients in a direct manner. These measurements will be discussed in detail in the following sections. By combining these results with the data from the coulex experiment, we will also be able to deduce the monopole transition strengths ρ(E0) of the E0 transitions.

2 Physics questions and the proposed experiment

2.1 ^{182}Hg

The previous β-decay studies [5] allowed to measure the branching ratios of the transitions from many of the low-lying states in ^{182}Hg. However, the uncertainties of some branching ratio values are relatively high (over 30%). The precise knowledge of these values is important, especially for the analysis of the data from the coulex experiments when calculating the reduced matrix elements, where a set of matrix elements is fitted to the measured γ-ray intensities depopulating Coulomb excited states. Calculations are performed using the coupled-channel least-square search code GOSIA [16, 17]. Deduced matrix elements usually occur as strongly correlated parameters in the fit of the coulex γ-ray intensities, thus additional spectroscopic data, such as branching ratios play an important role in constraining the number of the degrees of freedom in the analysis. Thus we propose to study these branchings in more detail.

The decay of the 2_2^+ state (see the level scheme in fig.2(left)) proceeds via three paths:

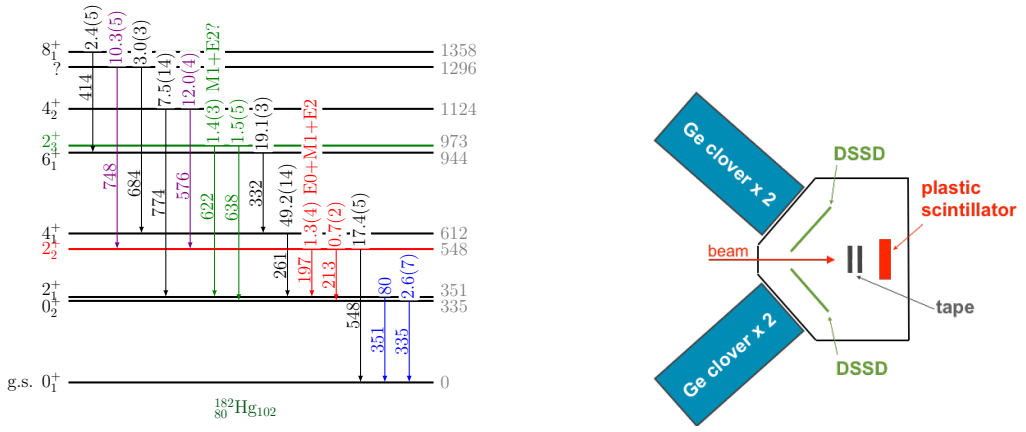

Figure 2: (Left) The simplified level scheme of ^{182}Hg. The relative intensities are normalised to the total ground state feeding; the excitation energies are given in keV [5]; (Right) A schematic view of the experimental setup (as seen from above)

the assumed "in-band" 213 keV $2_2^+ \rightarrow 0_2^+$ transition, the 548 keV $2_2^+ \rightarrow 0_1^+$ transition to the ground state and the 197 keV $2_2^+ \rightarrow 2_1^+$ transition known to have mixed E0/M1/E2 multipolarity. An E0 component present in the latter ΔI=0, $I \neq$0 transition could be interpreted as a measure of the mixing between the weakly oblate and the prolate-deformed

configuration components in the 2_1^+ and 2_2^+ levels and their difference in deformation.
Although the relative γ-ray intensities of the 548, 213 and 197 keV transitions were measured [5], the uncertainties on the last two branchings are higher than 30%. The precise information on these branching ratios is crucial for the determination of the quadrupole moments of the 2_1^+ and 2_2^+ states in GOSIA analysis. We thus propose to improve the precision of this number by gating on the 748 and 576 keV transitions and requiring a γ-γ coincidence. Within the requested beamtime, we expect to detect $1.9{\cdot}10^5$ γ-γ coincidences for the 197 keV transition and $1.1{\cdot}10^5$ for the 213 keV transition. The efficiency of the detection setup is given in section 3.
As the $2_2^+ \rightarrow 2_1^+$ transition also contains a converted component, we propose to take the ICE spectra with the silicon strip detectors and thus to determine the ICC as a ratio of the 197 keV γ-ray intensity and K-, L- and M-ICE intensities. The ICC value for this transition measured in [5] is 7.1(13), having a significant error bar which needs to be improved. Both γ and ICE parts of this transition can be isolated in a triple coincidence by gating on the 576 and 748 keV transitions feeding the 2_2^+ level and demanding a coincidence with the 351 keV transition depopulating the 2_1^+ level. This way we expect to detect $\sim 8{\cdot}10^4$ ICE and $\sim 1.4{\cdot}10^4$ γ-rays within the requested beam time. The K-shell ICC for this transition can also be obtained from the ratio of the γ-rays and the K X-rays stemming from this transition as a cross-check.
The 213 keV transition was not observed in [5] neither in singles nor in γ-γ coincidences, however its intensity was deduced from the coincidence of the 576 keV γ-ray to the K-shell ICE from the 335 keV E0 transition. Thus observing this transition with more statistics, with less background for the ICE and in absence of the γ-ray summing will improve the precision of the branching ratio determination.
The 2_3^+ level at 973 keV is supposedly a band-head of the γ-vibrational band built on top of the deformed band. It has a specific decay pattern, also observed in ^{184,186}Hg as shown in fig.1, only feeding 0_2^+ and 2_1^+ levels, while no transitions to the ground state or to the 2_2^+ state have been observed. The intensities of the 622 and 638 keV lines are 1.4(3) and 1.5(5) respectively. Reducing these uncertainties and detecting or setting upper limits on the de-excitation of the level towards the 2_2^+ and 0_1^+ states is essential for the analysis of the data from the future coulex experiment with HIE-ISOLDE, where the beam energy would be sufficient for the population of the 2_3^+ level. Moreover, it is useful to verify if the decay modes depopulating the 2_3^+ state contain converted components. It is known that the $2_3^+ \rightarrow 2_1^+$ in ^{186}Hg contains M1 and E2 components [18] (see subsection 2.3), but no such mixing was yet measured for the same transition in ^{182}Hg. According to [19], the γ-vibrational bands usually built on the prolate-deformed states are characterised by the enhanced $B(\mathrm{E2})$ strengths of the 2^+ to 0^+ transitions. Thus, quantifying the transition strengths of the $2_3^+ \rightarrow 0_2^+$ and $2_3^+ \rightarrow 2_1^+$ would provide information on the deformation of these levels. The high thickness of the silicon detectors will allow us to detect the ICE corresponding to the decay of the 2_3^+ state and thus to measure the corresponding ICC. The mutipole mixing ratio may be deduced from the ratio of the K- and L-conversion lines, which is 6.11 for the M1 multipolarity and 4.11 for the pure E2 transitions and typically around 5.8 for the E0 transitions in the lead region [20].

2.2 ^{184}Hg

Similar to ^{182}Hg, although ^{184}Hg was studied in the previous β^+/EC decay experiment, the uncertainties on some of the branching ratios and on the ICE intensities of the $2_2^+ \rightarrow 2_1^+$ transition are very large [5]. Similar levels as in ^{182}Hg will thus be studied by applying the same strategy.
In our experiment we propose to use narrow-band LI to $1/\lambda$=18058.8..18059.0 cm^{-1} frequencies (see fig.1 in [21]) in order to enhance the relative production of the (2^-) level in thallium by reducing the (10^-) production.

2.3 ^{186}Hg

The β^+/EC decay studies of ^{186}Tl [22] allowed to establish the level scheme of ^{186}Hg and to determine the relative branching ratios of the transitions as well as to measure many of the conversion coefficients and mixing ratios.
The hyper-fine structure of the high-spin β-decaying states in ^{186}Tl was studied in [23] by means of laser spectroscopy. The non-yrast low-spin states are weakly fed; however, α-decay of ^{190}Bi gives evidence that there is a low-spin (2^-) β-decaying isomeric state in ^{186}Tl [24] which was not yet studied in laser spectroscopy. Similar as for the ^{184}Tl, we will attempt to tune the laser to this (2^-) state.
As mentioned in section 2.1, the 2_3^+ level, the supposed band-head of a γ-vibrational band, shows decay behaviour similar to that in ^{182}Hg and ^{184}Hg: it was observed to decay to the 2_1^+ and 0_2^+ states only. The 691 keV transition (see fig.1(right)) was determined from the angular correlations to have a mixed M1+E2 multipolarity with a rather imprecise mixing ratio of $3.4^{+6.1}_{-1.8}$ [18]. We would like to measure the ICC for this transition from the ratio of the ICE and γ-ray intensities and to deduce the E0/M1/E2 mixing ratio from it. As the production rate of ^{186}Tl is very high, we will only require a few hours to study ^{186}Hg.

3 Description of the experimental setup

We propose to employ the combined γ-ray and ICE spectroscopy to study the ^{182,184,186}Hg isotopes produced in β^+/EC decay of ^{182,184,186}Tl. For the production of thallium, surface and laser ionisation on a UC_x target will be employed. We take conservative estimates of 1.75 pμA for the proton current and 50% for the RIBs transmission to the IDS. The expected thallium production rates are given in tab.1.

Isotope	Yield, ions/μC	BR$_{\beta^+/\mathrm{EC}}$	Rate at IDS, ions/s
^{182}Tl	$3.2{\cdot}10^4$	99.51%	$2.8{\cdot}10^4$
^{184}Tl	$1.7{\cdot}10^6$	98.78%	$1.5{\cdot}10^6$
^{186}Tl	$3.3{\cdot}10^7$	99.4%	$2.9{\cdot}10^{6\,*}$

Table 1: Expected production rates of the thallium isotopes. The yields are taken from the ISOLDE yields data base. *The ^{186}Tl rate at IDS is decreased in order to avoid the the pile-up.

The thallium beams will be implanted onto a mylar tape of the IDS tape station. The implantation point will be surrounded with 4 germanium clover detectors in a standard

IDS setup and two 1000 μm thick 5x5 cm 16x16 strips Double-sided Silicon Strip Detectors (DSSD) [25] (see fig.2(right)). A plastic scintillator detector will be placed behind the tape in order to provide a tag on the β^+ decay of thallium. The DSSDs will be cooled with liquid nitrogen via radiative exchange in order to reduce the thermal noise on the detector and thus to achieve the energy resolution of $\sim$7 keV for the ICE. The two clover detectors equipped with thin Be windows will allow the detection of the K X-rays of mercury. We expect to have an efficiency of 7.5% at 1 MeV for the γ-rays and a 10% of 4π solid angle coverage for the DSSDs [26].

4 Beam request

To fulfil our experiment we will need 2.5 shifts of the ^{182}Tl beam, 1 shift of the ^{184}Tl, 0.5 shift of the ^{186}Tl beam and 1 shift for the beam tuning.

Summary of requested shifts: *In total we request 5 shifts of Tl beam to fulfil the proposed program.* We request UC_x target and the RILIS ion source.

References

[1] K. Heyde, J. L.Wood, Rev. Mod. Phys. 83, (2011) 1467
[2] A. Gade, S.N. Liddick, J. Phys. G: Nucl. Part. Phys. 43, (2016) 024001
[3] J.L. Wood, E.F. Zganjar, C.D. Coster, K. Heyde, Nucl. Phys. A 651, (1999) 323
[4] L.P. Gaffney et al., Phys. Rev. C 89, (2014) 024307
[5] E. Rapisarda et al., accepted to J. Phys. G
[6] J. Bonn, G. Huber, H.-J. Kluge, L. Kugler, E. Otten, Phys. Lett. B 38, (1972) 308
[7] B. Marsh et al., to be published
[8] J.M. Yao, M. Bender, P.-H. Heenen, Phys. Rev. C 87, (2013) 034322
[9] L. Prochniak and G. Rohozinski, J. Phys. G 36, (2009) 123101
[10] K. Wrzosek-Lipska et al., Phys. Rev. C 86, (2012) 064305
[11] N. Bree et al., Phys. Rev. Lett. 112, 16 (2014), 162701
[12] K. Wrzosek-Lipska, to be published
[13] A.N. Andreyev et al., Phys. Rev. Lett. 105, (2010) 252502
[14] A.E. Barzakh et al., Phys. Rev. C 95, (2017) 014324
[15] C. Van Beveren et al., J. Phys. G: Nucl. Part. Phys. 43 (2016), 025102
[16] M. Zielinska et al., Eur. Phys. J. A 52 (2016), 99
[17] T. Czosnyka, D. Cline, and C. Y. Wu, Bull. Am. Phys. Soc. 28, 745 (1983).
[18] J.P. Delaroche et al., Phys. Rev. C 50 (1994), 5
[19] A. Bohr, R. Mottelson, "Nuclear structure", vol.2, W. Sci. Publ. Pte. Ltd., 1998
[20] W.H. Trzaska et al., Z. Phys. A 335, (1990) 475
[21] C. Van Beveren et al., Phys. Rev. C 92 (2015), 014325
[22] Evaluated Nuclear Structure Data File (ENSDF) (2017) *http://nndc.bnl.gov/ensdf*
[23] A.E. Barzakh et al., Phys. Rev. C 88, (2013) 024315
[24] P. Van Duppen et al., Nuc. Phys. A 529(1991) 268
[25] U.C. Bergmann et al., Nuc. Instr. Meth. A 515 (2003) 657
[26] M.V. Lund et al., Eur. Phys. J. A 52 (2016) 304

Appendix

DESCRIPTION OF THE PROPOSED EXPERIMENT

The experimental setup comprises: *IDS, RILIS*

Part of the	Availability	Design and manufacturing
(if relevant, name fixed ISOLDE installation: COLLAPS, CRIS, ISOLTRAP, MINIBALL + only CD, MINIBALL + T-REX, NICOLE, SSP-GLM chamber, SSP-GHM chamber, or WITCH)	☒ Existing	☒ To be used without any modification
[Part 1 of experiment/ equipment]	☐ Existing	☐ To be used without any modification ☐ To be modified
	☐ New	☐ Standard equipment supplied by a manufacturer ☐ CERN/collaboration responsible for the design and/or manufacturing
[Part 2 of experiment/ equipment]	☐ Existing	☐ To be used without any modification ☐ To be modified
	☐ New	☐ Standard equipment supplied by a manufacturer ☐ CERN/collaboration responsible for the design and/or manufacturing
[insert lines if needed]		

HAZARDS GENERATED BY THE EXPERIMENT (if using fixed installation:) Hazards named in the document relevant for the fixed [COLLAPS, CRIS, ISOLTRAP, MINIBALL + only CD, MINIBALL + T-REX, NICOLE, SSP-GLM chamber, SSP-GHM chamber, or WITCH] installation.

Additional hazards:

Hazards	[Part 1 of experiment/ equipment]	[Part 2 of experiment/ equipment]	[Part 3 of experiment/ equipment]
Thermodynamic and fluidic			
Pressure	[pressure][Bar], [volume][l]		
Vacuum			
Temperature	[temperature] [K]		
Heat transfer			
Thermal properties of materials			
Cryogenic fluid	[fluid], [pressure][Bar], [volume][l]		
Electrical and electromagnetic			

Electricity	[voltage] [V], [current][A]		
Static electricity			
Magnetic field	[magnetic field] [T]		
Batteries	□		
Capacitors	□		
Ionizing radiation			
Target material [material]			
Beam particle type (e, p, ions, etc)			
Beam intensity			
Beam energy			
Cooling liquids	LN_2 for cooling the Si detectors		
Gases	[gas]		
Calibration sources:	□		
• Open source	□		
• Sealed source	□ [ISO standard]		
• Isotope			
• Activity			
Use of activated material:			
• Description	□		
• Dose rate on contact and in 10 cm distance	[dose][mSV]		
• Isotope			
• Activity			
Non-ionizing radiation			
Laser			
UV light			
Microwaves (300MHz-30 GHz)			
Radiofrequency (1-300 MHz)			
Chemical			
Toxic	[chemical agent], [quantity]		
Harmful	[chem. agent], [quant.]		
CMR (carcinogens, mutagens and substances toxic to reproduction)	[chem. agent], [quant.]		
Corrosive	[chem. agent], [quant.]		
Irritant	[chem. agent], [quant.]		
Flammable	[chem. agent], [quant.]		

Oxidizing	[chem. agent], [quant.]		
Explosiveness	[chem. agent], [quant.]		
Asphyxiant	[chem. agent], [quant.]		
Dangerous for the environment	[chem. agent], [quant.]		
Mechanical			
Physical impact or mechanical energy (moving parts)	[location]		
Mechanical properties (Sharp, rough, slippery)	[location]		
Vibration	[location]		
Vehicles and Means of Transport	[location]		
Noise			
Frequency	[frequency],[Hz]		
Intensity			
Physical			
Confined spaces	[location]		
High workplaces	[location]		
Access to high workplaces	[location]		
Obstructions in passageways	[location]		
Manual handling	[location]		
Poor ergonomics	[location]		

Hazard identification:

Average electrical power requirements (excluding fixed ISOLDE-installation mentioned above): [make a rough estimate of the total power consumption of the additional equipment used in the experiment]